

Electrochemical Reversibility of Reticulated Vitreous Carbon Electrodes Heat Treated at Different Carbonization Temperatures

Emerson Sarmento Gonçalves^{a,b,*}, Mirabel Cerqueira Rezende^a,

Marta Ferreira Koyama Takahashi^c, Neidenêi Gomes Ferreira^d

^aDivisão de Materiais, AMR/IAE/CTA, Centro Técnico Aeroespacial

^bDepartamento de Aeronáutica e Mecânica, ITA/CTA, Centro Técnico Aeroespacial

^cDivisão de Química, AQI/IAE/CTA, Centro Técnico Aeroespacial,
12228-904 São José dos Campos - SP, Brazil

^dLaboratório Associado de Sensores, CTE/INPE, Instituto Nacional de Pesquisas Espaciais,
12227-010 São José dos Campos - SP, Brazil

Received: February 14, 2005; Revised: March 9, 2006

Electrochemical response of ferri/ferrocyanide redox couple is discussed for a system that uses reticulated vitreous carbon (RVC) three dimensional electrodes prepared at five different Heat Treatment Temperatures (HTT) in the range of 700 °C to 1100 °C. Electrical resistivity, scanning electron microscopy and X ray Diffraction analyses were performed for all prepared samples. It was observed that the HTT increasing promotes an electrical conductivity increasing while the Bragg distance d_{002} decreases. The correlation between reversibility behavior of ferri/ferrocyanide redox couple and both surface morphology and chemical properties of the RVC electrodes demonstrated a strong dependence on the HTT used to prepare the RVC.

Keywords: *reticulated vitreous carbon, pyrolysis, X ray diffraction, electrochemical properties*

1. Introduction

Reticulated Vitreous Carbon (RVC) is an important material known by its high mechanical resistance, porosity, biocompatibility and relatively high electrical conductivity. These properties have been extensively explored in the last decades in many applications, for example, in thermal coating of aerospace vehicles^{1,2}, bony prostheses³, heart valves^{4,6}, molecular sieves⁷ and hydrogenation catalyst supports⁸.

Electrical conductivity variation is a determinant parameter for using RVC electrodes in many electrochemical applications. Polyaromatic hydrocarbon crystals are intrinsic semi-conductors with resistivity values between 10^2 and 10^{10} Ω .cm. RVC characteristically shows a decrease in its electrical resistivity as a function of the manufacturing temperature increase. This behavior is associated with a better arrangement of the carbon atoms in the basal planes, forming graphitic lamellar planes, which are stacked in the carbon structure. This graphitic structure favors the transference of electrons among the hexagonal carbon rings in carbon material⁹. The extreme case of a polyaromatic carbon material highly arranged is the graphite single crystals. The carbon plane sheets show two-dimensional metallic conduction with resistivity values smaller than 3.3×10^{-5} Ω .cm within the sheet and a negative temperature coefficient⁹. The gradual increase of conjugated carbon in the sp^2 state during the heat treatment of the raw material in inert atmosphere (carbonization treatment) changes the precursor material progressively from an insulator to a good conductor in a remarkable decrease of 19 orders of magnitude in resistivity values. The electrical property is, therefore, sensitive to measure the various stages of the carbonization treatment and provide information about the final structure of carbon⁹. Yamaguchi¹⁰⁻¹² made the first measurements of electrical resistivity of vitreous carbon obtained from heat treatment temperatures between 800 °C and 3200 °C.

The electrical resistivity behavior of vitreous carbon derived from phenolic resin, at room temperature, assessed by potentiometric method, was described by Jenkins et al.⁹. The resistivity decreases rapidly up to 900 °C. Afterwards, it decreases gradually reaching a constant value at 1500 °C, comparable to that of well-graphitized material with crystallite size greater than 1000 Å.

Additionally, the literature shows that the conductivity of solid carbons reaches a similar value in the same temperature range, between 600 °C and 700 °C, when the carbon loses its acid properties¹³⁻¹⁸. The properties of solid carbon surface are strictly related to heteroatoms, which are removed during the heat-treatment, as water (up to 400 °C), CO₂ (up to 700 °C), CO (up to 1200 °C), H₂ and CH₄ (above 950 °C), and also nitrogenated and sulfonated forms (above 1800 °C)^{13-15,19-23}. Therefore, the acid functionality loss (initially by CO₂) approximately coincides with the trend of electrical conductivity to keep nearly constant for solid carbons. These factors are presumably related to the effects of electron delocalization, which favors electrical conduction that becomes higher after the acid group loss.

Furfuryl alcohol resin is a polymer of national production and it usually presents low volatile losses during curing and carbonization processes. These characteristics induce to the more dense final carbonized foam (RVC) stems and, consequently, with higher mechanical properties (for example more resistant to flexion efforts) and lower electrical resistivity than those obtained from phenolic resins.

This work aims to systematically describe the morphological and structural properties of RVC three dimensional electrodes, produced from furfuryl alcohol resin at different HTT, by SEM and XRD measurements. Electrical resistivity of RVC samples is also correlated with its electrochemical response, evaluating the reversibility behavior for the ferri/ferrocyanide redox couple.

*e-mail: sarmgon@yahoo.com

2. Experimental

RVC was obtained by impregnation of a polyether based polyurethane (PU) foam, commercially available, by using furfuryl alcohol resin (dynamic viscosity of ~ 3.0 Pa s). Using p-toluenosulfonic acid as catalyst (3% w/w) the resin cure process was carried out. Furfuryl alcohol resin cure cycle was performed at 60 °C and this temperature was kept for 2 hours. Afterwards, the temperature was raised up to 80 °C for 2 hours. Then, the samples show suitable mechanical resistance to be manipulated and machined in different shapes.

To evaluate the influence of the maximum HTT on the RVC properties the cured resin was carbonized up to five different maximum temperatures, between 700 °C and 1100 °C. The samples were heated at 1.0 °C min⁻¹ under a nitrogen flow of 1 L.h⁻¹, from room temperature until the selected maximum temperature. This step took nearly 30 minutes. The cooling occurred naturally up to room temperature.

The RVC superficial morphology analyses were performed by Scanning Electronic Microscopy (SEM) by using the equipment Zeiss DSM/950. Structural analyses were carried out by X ray Diffraction (XRD) in a diffractometer Phillips, PW 1210/W/380/80.

Electrical resistivity measurements were carried out according to the four-probe method²⁴. The samples were kept linked to a tension measurer HP 34401A and a continuous current generator Tectrol TC-50-015. RVC samples were shaped into rectangular bars with the longest axis being the axis of the resistivity measurements. Silver paint was used for improving the electrical contacts. The compact volume electrical resistivity (ρ) was determined as a function of the inner probe separation.

FTIR (Fourier Transformed Infrared) spectra were performed by using a spectrophotometer SPECTRUM 2000 – Perkin Elmer, in the region of 4000 - 400 cm⁻¹. The spectra were obtained by Photoacoustic Spectroscopy (PAS) technique.

Cyclic Voltammetry (CV) measurements were carried out by using a Microquímica potentiostat MQPG-01 in 1 mM of ferrocyanide/0.1 M KCl, at scan rates of 5 to 500 mV.s⁻¹. The experiments were performed at room temperature in normal atmosphere. A simple three-electrode (WE – Working Electrode, CE – Counter Electrode of Pt mesh, RE – Reference Electrode of Ag/AgCl) and a single-compartment electrochemical cell were used in this study. The CE was positioned in front of the WE one. The RE was positioned close to the WE one, in the opposite side of the CE. The WE was prepared by machining RVC pieces in rectangular shape with dimensions of 14.3 mm x 12.6 mm x 7.02 mm, respectively. For all experiments, the RE was Ag/AgCl. The solution was not stirred during the voltammetry experiments. The end of the electrodes was assembled over one brass base and the electrical contact was adapted by using silver based paste to improve the electrical contact. The electrodes were not submitted to superficial pre-treatment before the electrochemical measurements and their behaviors were registered in the first CV cycle.

3. Results and Discussion

3.1. Morphology and microstructure

Images obtained by SEM do not reveal large differences among the RVC structures manufactured at different HTT. However, the bubble formation is remarkable in the temperature range of 700 °C and 800 °C, as shown in Figure 1a,b. SEM images of the RVC samples, with magnification of 20 times, (Figure 1c) allow estimating the pore diameters and its distribution considering pores per inch (ppi). This figure shows that the RVC is rich in transport pores with robust stems that guarantees its handling. Figure 1d depicts a small region of the vitreous carbon stem treated at 1100 °C. This typical image shows a smooth aspect of the vitreous carbon and no bub-

ble presence. Generally speaking, the manufactured RVC presents macropores with average diameter of 460 μ m, which correspond to around 50 ppi. This value is important to estimate the specific geometric surface area of electrode. Friedrich et al.²⁵ measured the effective area of the pore stems by SEM and found a linear relation between the quantity of ppi and the specific surface area. By using this relation a specific area of 31.0 cm² cm⁻³ was evaluated for the 50 ppi-RVC sample tested in this work.

Figure 2 presents the resistivity behavior as a function of HTT. This analysis is commonly presented in literature⁶, but it does not involve the electrochemical response of the electrodes. In Figure 2 an abrupt decrease of the resistivity values is observed. This value is nearly ten times higher for the RVC sample treated at 700 °C than the one treated at 800 °C. Above this temperature (up to 1100 °C) the resistivity values show no significant variation. Usually, to explain these results, the classical approach used for semiconductor conductivity is applied²⁶. This consideration is associated with the presence of energy gaps of two different origins, i.e., the intrinsic gap and one caused by impurities or lattice defects attributed to crystalline structure distortions. The later, as a chemical effect, decreases as the temperature increases and it is correlated to the fact that lower HTT does not offer sufficient energy for eliminating bonds C = C and functional groups C = O. The presence of these functionalities on the RVC surface (C = C and C = O) was determined by FTIR analysis for the samples treated at 700 °C, as shown in Figure 3. This figure shows contributions of C = C and C = O at 1700 - 1500 cm⁻¹. The presence of an intrinsic gap is explained by graphite-like ribbon distortions. Additionally, the bubbles present in Figure 1a,b, which represent vacancies, can also promote the conductivity decrease.

X ray diffraction measurements have proved to be an important technique for RVC structural analysis. Considering the model proposed by Kawamura and Jenkins²⁷ for vitreous carbon structure, the main purpose of these measurements is to evaluate both the development of carbon layers²⁸ and the character of their mutual ordering²⁹. It is known that the profiles of (*hk*) reflections correspond to the model of flat rectangular anisotropic Coherently Scattering Domains (CSD). The heat treatment results in anisotropic growth of CSD²⁹. Figure 4 shows the determined values for both the distances between the lamellar planes (d_{002}) and the plane stacking sizes (L_{002}) evaluated from XRD spectra. The analysis of (002) reflections evidences a sharp reduction of interlayer distance from 0.377 nm to 0.364 nm between 700 °C and 1100 °C. These results may be explained from two important contributions. The first involves the volatile release trapped in the material and the second the rearrangement of graphitic lamellar planes. The simultaneous occurrence of these two phenomena leads to a more organized carbon structure, as described in literature⁹. In this same temperature interval L_{002} changes from 0.698 nm up to 0.848 nm, confirming the crystallinity increase as a function of the HTT. This is related to the repulsive interaction decrease between the clouds of π -electrons of adjacent graphitic layers, allowing these layers to come closer. In fact, the release of both oxygenated groups and olefin bonds provides a decrease in the electronic cloud density, responsible for the repulsion among layers. Besides, these groups and bonds represent a volumetric impediment which leads to the Bragg distance decreasing. This interpretation confirms the mechanism proposed by Fitzer et al.^{31,32}.

3.2. Electrochemical behavior

Cyclic voltammetry analysis has been widely used to characterize different types and shapes of carbon electrodes^{9,13}. A series of experiments was carried out to study the electrochemical behavior of RVC electrodes in ferrocyanide redox couple. The main objective was to

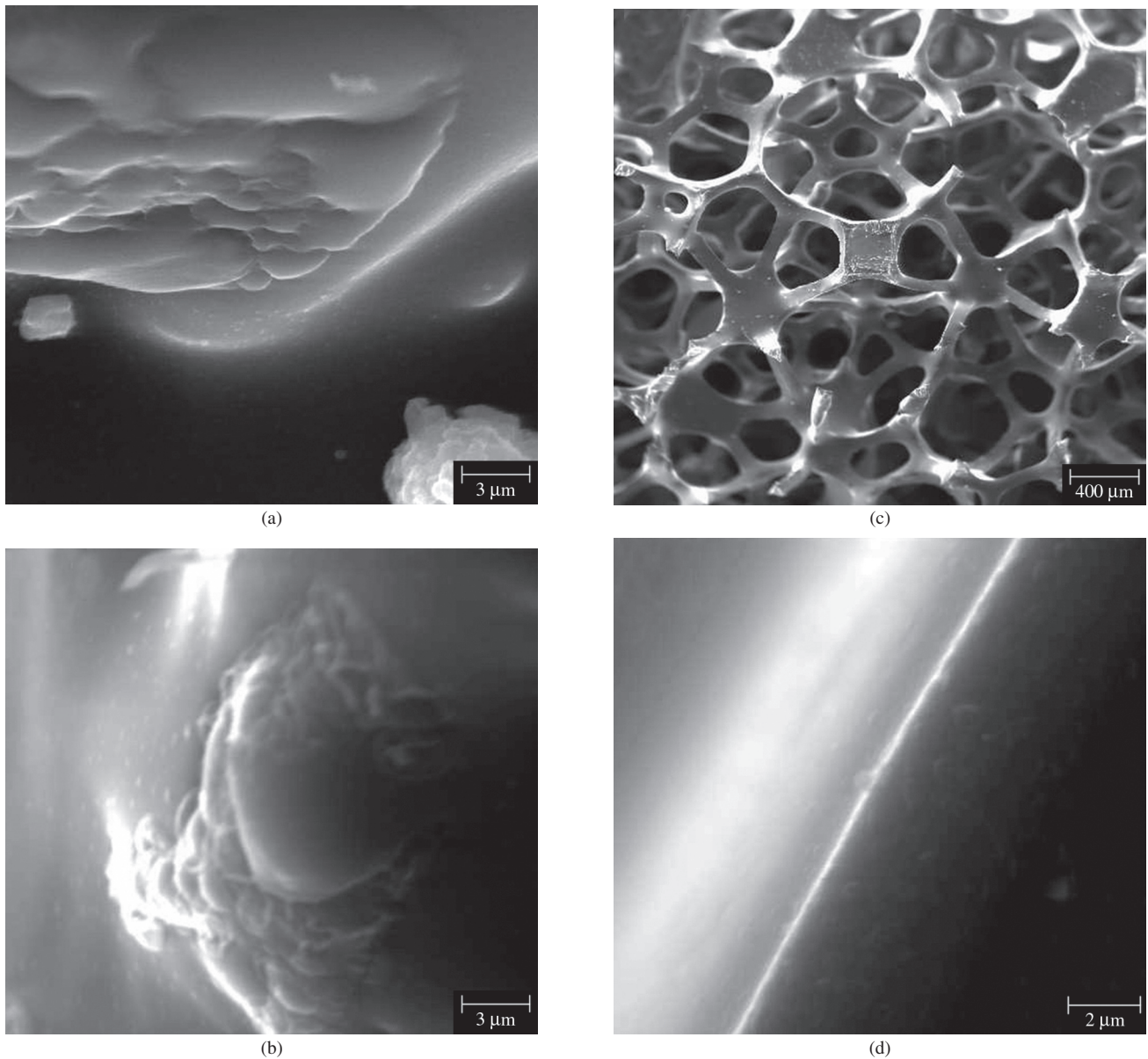


Figure 1. SEM images of RVC samples heat treated at: a) 700 °C-3000 X; b) 800 °C-3000 X; c) 800 °C-20 X; and d) 1100 °C-5000 X.

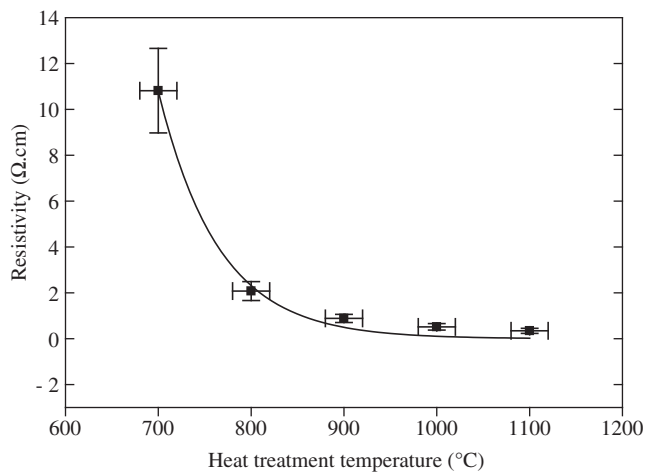


Figure 2. Resistivity behavior of RVC as function of the maximum temperature used in its manufacture.

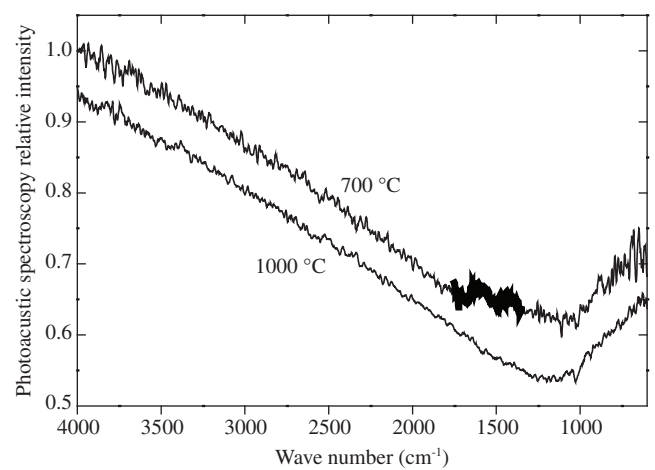


Figure 3. FT-IR spectra of RVC samples heat treated at 700 °C and 1000 °C. The interval between 1700 and 1100 cm^{-1} suggest the presence of functionalities. The relevant contributions are marked in spectrum.

verify the electrode response agreement using some criteria of *quasi* reversibility for the usual redox reactions in this electrolyte³³. The correlation between morphological and structural results previously discussed and the voltammetric data supports the consistency of this study. Electrochemical response also permitted to evaluate the Specific Electrochemical Surface Area (SESA) of the RVC electrodes. The results have shown a strong dependence between the HTT and the reversibility behavior, as expected. This method represents an additional technique for controlling the RVC electrode quality. To understand the next approach, the following notion was used: S_s for the specific surface area ($\text{cm}^2 \text{cm}^{-3}$); I_p for the anodic peak current intensity (A); C_o for the oxidant concentration (equal to reductor); V_{el} for the electrode volume immersed in solution (cm^3); D_o for the oxidant diffusivity in solution ($\text{cm}^2 \text{s}^{-1}$, also considered equal to reductor), and v for the sweeping rate in voltammetric experiments (V.s^{-1}).

The voltammetric studies show that the RVC electrodes may be analyzed by quasi-reversibility criteria: I_p increases with $v^{1/2}$ but does not keep the proportionality; ΔE_p is larger than $59/n$ mV and it increases with v ; and the cathodic peak potential, E_{pc} , shifts to negative value when v increases. This analysis was associated with the kinetic parameters ΔE_p and I_{pc} as function of both HTT and sweeping rate³³. The treatment of systems called quasi-reversible is associated with reactions that show electron transfer kinetic limitations where the reverse reaction must be considered. The results obtained in the performed experiments led to conclude that this consideration is the most suitable treatment for such RVC electrodes in the studied redox system, mainly due to the range of ΔE_p obtained as a function of the sweeping rates.

Figure 5 presents voltammetric curves for a RVC electrode treated at 800 °C in 1 mM of ferrocyanide/0.1 M KCl. For all electrodes, it was observed that the sweeping rate increase promotes an increase of the current peak intensity in cathodic and anodic reactions. The

anodic peak shifts from 0.290 V to 0.420 V and the cathodic peak shifts from 0.24 V to 0.0752 V. Only some curves are shown for a better visualization.

The anodic peak current is also used to evaluate the specific electrochemical surface area, which is obtained by Equation 1³⁴:

$$\text{SESA} = \frac{I_p}{2.69 \times 10^5 C_o V_{el} \sqrt{D_o v}} \quad (1)$$

where: SESA values are shown in Figure 6. These values are in good agreement with Friedrich et al.²⁵, for samples heat treated at temperatures of 1000 °C and 1100 °C, considering the area measurements of the foam stems. The apparent disagreement for lower HTT samples may be explained by two important contributions. The lower HTT provides larger resistive effect as exposed in Figure 2, which is determinant for the electrode electrochemical response. Besides, the influence of the measured current may also contain an unknown contribution from surface modifications of the electrode³⁴. FTIR analysis supports this argument by detecting carbonyl groups and olefin bonds that represent modifications on carbon surface for samples heat treated at 700 °C. The micrometric bubbles observed by SEM are an additional factor which may represent important roughness effect. Consequently, the surface

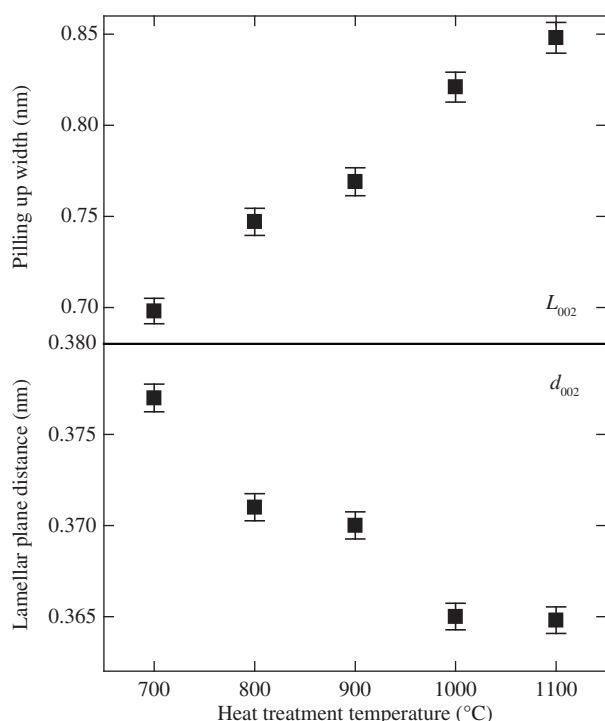


Figure 4. Lamellar planes d_{002} and pilling up width L_{002} obtained from XRD analysis.

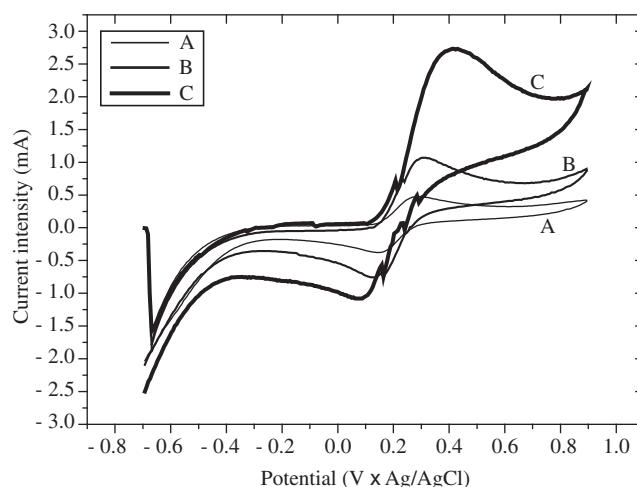


Figure 5. Cyclic voltammetric behavior of RVC electrode heat treated at 800 °C in 1 mM Ferrocyanide/0.1 M KCl. Each voltammogram is related to one sweep rate: A = 5 mV.s^{-1} ; B = 50 mV.s^{-1} ; and C = 500 mV.s^{-1} .

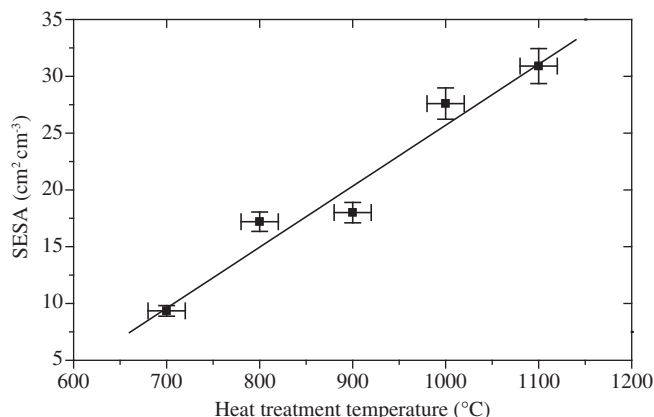


Figure 6. Specific electrochemical surface areas (SESA) for RVC electrodes manufactured at different HTT (from 700 °C up to 1100 °C).

area value evaluated through this process will not represent the real area of such electrode.

By using the quasi-reversibility criteria, ΔE_p shows a slightly increase (for the samples heat treated at 800 - 1100 °C) with the sweeping rate increase and it is larger than $59/n$ mV (where $n = 1$ is the number of electrons involved in the reaction) (Figure 7), assisting an approach of *quasi* reversibility. Another important aspect is related to the cathodic peak variation: the current increases with $v^{1/2}$, as shown in Figure 8. From this figure it is possible to observe the irreversibility of the system assembled with RVC electrodes heat-treated at the maximum temperature of 700 °C. This is observed by considering that the peak current profile does not increase in function of $v^{1/2}$ if compared with the pronounced increase observed for the RVC electrodes treated at higher temperatures. The carbonyl groups and olefin bonds determined by FTIR analysis for the samples heat treated at 700 °C, associated to the bubble presence on the steam surfaces, justify this significant difference observed for the electrochemical behavior of such samples. Firstly, the bubbles provide an increase of the void volume that hinders the electron transport. Also, the presence of oxygenated groups such as carbonyl, carboxyl, lactones and quinones is related in literature³⁵. Presence of methilencial bonds decreases the conductivity because it constitutes an electronic barrier from sp^3 hybridization. However, it is known that the presence of acid groups in samples does not necessarily provide resistivity changes, but decreases the cathodic character of vitreous carbon. Figure 9 reveals that ΔE_p is larger only for electrodes heat treated at 700 °C, indicating the inadequacy of this treatment for obtaining a good electrode. For HTT higher than 900 °C, ΔE_p is 0.2 V, nearly six times lower than that determined for the sample treated at 700 °C. This electrochemical behavior is similar in the whole range of sweeping rate studied.

4. Conclusions

RVC electrodes obtained from different heat treatment temperatures were studied by correlating their morphology, structure, electrical resistivity and electrochemical response. X ray diffraction and resistivity measurements have demonstrated to be important tools for studying the RVC electrode properties. Besides, electrochemical study has shown to be adequate for detecting electroactive species and revealing a quasi-reversible behavior for such electrodes, except for samples heat treated at 700 °C. This sample, which presents carbonyl groups, showed by cyclic voltammetry the lowest anodic and cathodic current peaks and the largest ΔE_p , mainly correlated to its higher resistivity. This effect provides voltammograms without peaks and with the highest inclination, revealing worthless faradic current peaks. Finally, the evaluation of the specific electrochemical area is strongly affected by the electrode resistivity. For the samples manufactured by using HTT values higher than 800 °C, with lower resistivity values, a SESA was found in good agreement with the values shown by Friedrich et al.²⁵. The resistive component of voltammograms in the temperature range of 700-800 °C is more intense for carbon treated at lower HTT, influencing the electrochemical responses. This behavior is probably related to the presence of methilencial bonds and oxygenated groups from furfuryl alcohol resin used as raw material in the RVC processing.

Acknowledgments

The authors would like to thank A. O. Santos for SEM images, A. V. Diniz from LAS/INPE for X ray diffraction measurements and FAPESP (Process number: 05/50718-9) and CNPq (Process number: 303528/2003-6). We are specially grateful to E. C. Botelho for improving the technical discussion of this work.

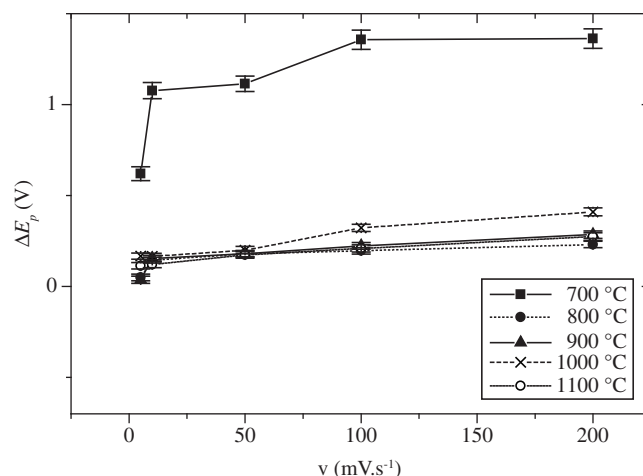


Figure 7. ΔE_p as a function of sweep rate in 1 mM Ferrocyanide/0.1 M KCl for RVC electrodes manufactured at different HTT (from 700 °C up to 1100 °C).

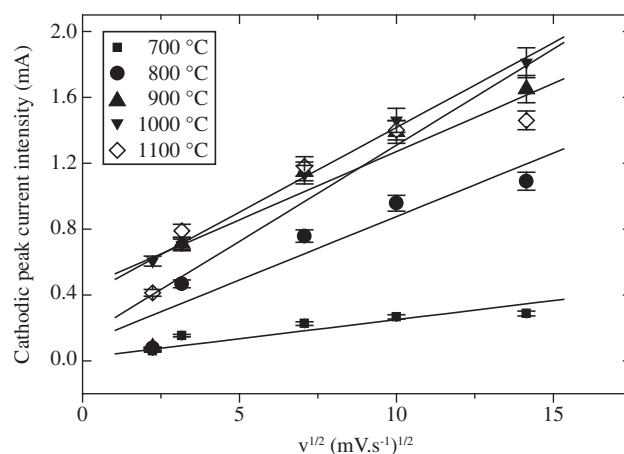


Figure 8. Cathodic peak current as a function of $(\text{sweep rate})^{1/2}$ in 1 mM Ferrocyanide/0.1 M KCl for RVC electrodes manufactured at different HTT (from 700 °C up to 1100 °C).

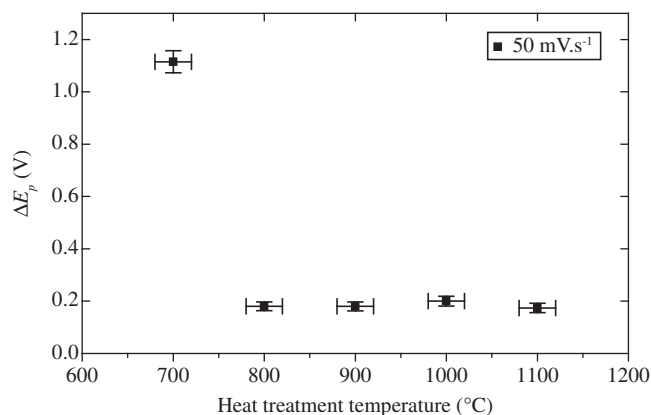


Figure 9. ΔE_p as a function of HTT used in the RVC electrode manufacture, in 1 mM Ferrocyanide/0.1 M KCl at sweep rate of 50 mV.s^{-1} .

References

1. Bradshaw WG, Pinoli PC, Mitchell MJ. Recent Developments in glassy carbon fabrication. In: *Proceedings of 9th Biennial Conference on Carbon; 1969; Boston: USA*. Boston: American Carbon Society; 1969. p. 7.
2. Bunnell LR. Proc. Vitreous carbon matrix carbon-carbon composite by copyrolysis. In: *Proceedings of 12th Biennial Conference on Carbon; Pennsylvania; 1975; USA*. Pennsylvania: American Carbon Society; 1975. p. 333-334
3. Kaplan RB. Open cell tantalum structures for cancellous bone implants and cell and tissue receptors. *US Patent* 5282861; 1994.
4. Rezende MC. *Produção de Carbono Vítreo, em Escala de Laboratório, a partir de Resinas Furfúrica e Fenólica. São Paulo: Brazil*. [Doctoral Thesis]. São Paulo, EPUSP; 1991.
5. Bokros JC. Carbon biomedical devices. *Carbon*. 1977; 15(6):353.
6. Jenkins GM, Grigson CJ. The fabrication of artifacts out of glassy carbon and arbon-fiber-reinforced carbon for biomedical applications. *J. Biomed. Mater. Res.* 1979; 13:371-394.
7. Schmitt Jr JL, Walker PL. Carbon molecular sieve supports for metal catalysts-II. Selective hydrogenation of hydrocarbons over platinum supported on polyfurfuryl alcohol. *Carbon*. 1972; 10(1):87-92.
8. Cooper BJ, Trimm DL. Selectivity of carbon molecular sieve supported catalysts. In: *Preprint 3rd Conference on Industrial Carbon and Graphite; 1970; London: UK*. London: Soc. Chem. Ind.; 1970. p. 49.
9. Jenkins GM, Kawamura K. *Polymeric carbons – carbon fibre, glass and char*. Cambridge: Cambridge University Press; 1976. p. 83-108
10. Yamaguchi T. Galvanomagnetic properties of glassy carbon. *Carbon*. 1964; 1(1):47-50.
11. Yamaguchi T. Thermoelectric power of glassy carbon at high temperature. *Carbon*. 1964; 1(4):535-536.
12. Yamaguchi T. Electronic Properties of Carbonized Polyacrylonitrile Fibers. *Carbon*. 1964; 2(1):95-96.
13. Leon y Leon CA, Radovic LR. Interfacial Chemistry and Electrochemistry of Carbon Surfaces. In: Throver PA, editor. *Chemistry and physics of carbon; New York: USA*. New York: Dekker. 1994; 24:213-310.
14. Rivin D. Surface Properties of Carbon. *Rubber Chem. Technol.* 1971; 44:307-343.
15. Rivin D. *Carbon Black Iodination. Extended Abstract, in Proc. 5th Conf. on Carbon; 1963; New York: USA*. New York: Pergamon Press; 1963. v. 2. p. 199.
16. Papirer E, Li S, Donnet JB. Contribution to the study of basic surface groups on carbons. *Carbon*. 1987; 25(2):243-247.
17. Papirer E, Dentzer J, Li S, Donnet JB. Surface groups on nitric acid oxidized carbon black samples determined by chemical and thermodesorption analyses. *Carbon*. 1991; 29(1):69-72.
18. Puri BR. Surfaces complexes on Carbons. In: Walker, Jr PL, editor. *Chemistry and physics of carbon; New York: USA*. New York: Dekker. 1970; 6:191-282.
19. Kinoshita K. *Carbon: Electrochemical and Physicochemical Properties*, New York: Wiley, p. 1-17, 86-91, 1988.
20. Morimoto T, Miura K. Adsorption sites for water on graphite. 1. Effect of high-temperature treatment of sample. *Langmuir*. 1985; 1(6):658-662.
21. Morimoto T, Miura K. Adsorption sites for water on graphite. 2. Effect of autoclave treatment of sample. *Langmuir*. 1986; 2(1):43-46.
22. Miura K, Morimoto T. Adsorption sites for water on graphite. 3. Effect of oxidation treatment of sample. *Langmuir*. 1986; 2(6):824-828.
23. Miura K, Morimoto T. Adsorption sites for water on graphite. 4. Chemisorption of water on graphite at room temperature. *Langmuir*. 1988; 4(6):1283-1288.
24. Shui X, Frysz CA, Chung DDL. Solvent cleansing of the surface of carbon filaments and its benefit to the electrochemical behavior. *Carbon*. 1995; 33(12):1681-1698.
25. Friedrich JM, Ponce-de-León C, Reade GW, Walsh FC. Reticulated vitreous carbon as an electrode material. *Journal of Electroanalytical Chemistry*. 2004; 561(1):203-217.
26. Pesin LA. Review – Structure and properties of vitreous carbon. *J. Matter. Sci.* 2002; 37:1-28.
27. Kawamura K, Jenkins GM. Structure of Glassy Carbon. *Nature*. 1971; 231:175-176.
28. Fischbach DB. The Kinetics and Mechanism of Graphitization. In: Walker, Jr PL, editor. *Chemistry and physics of carbon; New York: USA*. New York: Dekker. 1971; 7:1-105.
29. Rousseaux F, Tchoubar D. Structural evolution of a glassy carbon as a result of thermal treatment between 1000 and 2700 °C – I. Evolution of the Layers. *Carbon*. 1977; 15(2):55-61.
30. Hagio T, Nakamizo M, Kobayashi K. Studies on X-ray diffraction and Raman spectra of B-doped natural graphite. *Carbon*. 1989; 27(2):259-263.
31. Fitzer E, Schafer W, Yamada S. The formation of glasslike carbon by pyrolysis of polyfurfuryl alcohol and phenolic resin. *Carbon*. 1969; 7(6):643-646.
32. Fitzer E, Schafer W. The effect of crosslinking on the formation of glasslike carbons from thermosetting resins. *Carbon*. 1970; 8(3):353-364.
33. Greef R, Peat R, Peter LM, Pletcher D, Robinson J. *Instrumental Methods in Electrochemistry*, New York: Wiley; 1985. p. 178-227.
34. Trassatti S, Petrii OA. Real Surface Area Measurements in Electrochemistry. *Pure & Appl. Chem.* 1991; 5(5):711-734.
35. Fabish TJ, Schleifer DE. Surface chemistry and the carbon black work function. *Carbon*. 1984; 22(1):19-38.